Available online at www.easdprocedia.org
EASD Procedia EURODYN (2020) 1586-1612

EASD Procedia

EURODYN 2020
XI International Conference on Structural Dynamics
M. Papadrakakis, M. Fragiadakis, C. Papadimitriou (eds.)
Athens, Greece, 23–26 November 2020

EXPERIMENTAL STUDY OF RAILWAY BRIDGES OF SEVERAL STRUCTURAL TYPOLOGIES

P. Galvín[1], E. Moliner[2], A. Romero[1] and M.D. Martínez-Rodrigo[2]

[1] Escuela Técnica Superior de Ingeniería, Universidad de Sevilla
Camino de los Descubrimientos s/n, ES-41092 Sevilla, Spain
e-mail: {pedrogalvin,aro}@us.es

[2] Department of Mechanical Engineering and Construction, Universitat Jaume I
Avda. Sos Baynat s/n, ES-12071 Castellón, Spain
e-mail: {lola.martinez,molinere}@emc.uji.es

Keywords: Railway bridges, experimental measurements, traffic induced vibrations, bridge dynamics.

Abstract. *This work is devoted to the experimental evaluation of the dynamic response of railway bridges with common typologies in short-to-medium spans. An extensive experimental campaign is performed in several railway bridges belonging to the High-Speed (HS) and conventional Spanish railway network. The main objectives are to (i) characterise the structures main features affecting their dynamic behaviour, (ii) determining the soil properties at the structures respective locations; and analysing the bridge dynamic responses under different operating conditions. All the bridges are composed by simply-supported (S-S) bays with different steel, concrete and steel-concrete composite typologies. Five bridges have been experimentally investigated: i) Old Guadiana Bridge: a double-track simply-supported bridge with two $13\,m$ equal spans composed by two adjacent single-track decks with continuous ballast; ii) Jabalón High-Speed Bridge: an isostatic bridge of three S-S bays of $20\,m$ equal spans composed by a double-track pre-stressed concrete girders deck; iii) Algodor Bridge: an isostatic double-track bridge with three S-S bays of $10\,m$ equal spans and a pseudo-slab concrete deck; iv) Jabalón Conventional Line Bridge: a steel truss single-track structure composed by three $25\,m$ equal spans; and v) Tinajas Bridge: a steel-concrete composite single-track bridge with three bays of 25, 35 and $22\,m$ spans, respectively. The first four bridges are nowadays at full operation while the latter is under its construction final stage. The study includes the identification of bridge modal parameters and dynamic soil properties, a discussion on the identified structural damping in all the bridges, the measurement of vibration levels induced by railway traffic under operational conditions in the first four bridges and under construction operation machinery in the fifth case, and an analysis of the differences found in the structural behaviour of different bridge typologies for the same traffic. This paper summarizes a vast experimental campaign.*

ISSN:2311-9020 © 2020 The Authors. Published by EASD Procedia.
Peer-review under responsibility of the Organizing Committee of EURODYN 2020.
doi: 10.47964/1120.9129.18600

1 Introduction

The dynamic effects in railway bridges have become an issue of interest and concern for scientists and engineers in the last decades, especially since the advent of High-Speed [1]. An excessive level of vertical accelerations on the deck platform (greater than 3.5 or $5\,\mathrm{m/s^2}$ in ballast or slab track bridges, respectively), can lead to misalignment of the rails as a result of premature deconsolidation of the ballast layer, to the loose of contact between wheel and rail with the subsequent increase of the risk of derailment, to fatigue problems in the structures in the long term or to an increase of the maintenance costs in the best scenario. Consequently, the Serviceability Limit States for Traffic Safety and, in particular, the vertical acceleration of the deck has become one of the most restrictive requirements in the design of new bridges. The bridges composed by simply-supported spans with short to medium span lengths are especially critical in this regard, due to their natural frequencies and usually low mass and damping associated levels. This problem of high accelerations is particularly relevant at resonance [2, 3].

A comprehensive experimental campaign in five railway bridges in Spain is presented in this work. The tests include the identification of the modal parameters of the structures, the characterization of the soil at the respective sites and the measurement of the bridge dynamic responses under railway traffic. Five bridges were tested: $i)$ Old Guadiana Bridge: a double-track S-S bridge with two $13\,\mathrm{m}$ equal spans composed by two adjacent single-track decks sharing a continuous ballast layer; $ii)$ Jabalón High-Speed Bridge: an isostatic bridge with three S-S bays of $20\,\mathrm{m}$ equal spans composed by a double-track pre-stressed concrete girders deck; $iii)$ Algodor Bridge: a double-track bridge with three S-S bays of $10\,\mathrm{m}$ equal spans and a filler beam concrete deck; $iv)$ Jabalón Conventional Line Bridge: a steel truss single-track structure composed by three $25\,\mathrm{m}$ equal spans; and $v)$ Tinajas Bridge: a steel-concrete composite single-track continuous bridge with three spans of 25, 35 and $22\,\mathrm{m}$, respectively.

The outline of the paper is as follows. In Section 2, a general description of the experimental tests performed during the campaigns is included. The results of the experimental measurements on each particular bridge are given in the different subsections of Section 3. A final analysis on the differences found in the structural behaviour of the different typologies for similar traffic is included in Section 4.

2 Experimental set-up

In April and May 2019, the authors performed an experimental campaign on several railway bridges with the purpose of characterizing the structure and soil dynamic properties along with the bridge dynamic response under railway traffic. As per the acquisition equipment, a portable acquisition system LAN-XI of Brüel & Kjaer was used. The acquisition system fed the sensors (accelerometers) and an instrumented impact hammer in the case of the soil tests. It also performed the Analog/Digital conversion (A/D). The A/D was carried out at a high sampling frequency that avoided aliasing effects using a low-pass filter with a constant cut-off frequency. The sampling frequency was $f_s = 4096\,\mathrm{Hz}$. The acquisition equipment was connected to a laptop for data storage. Endevco model 86 piezoelectric accelerometers were used with a nominal sensitivity of $10\,\mathrm{V/g}$ and a lower frequency limit of approximately $0.1\,\mathrm{Hz}$. The acquisition system was configured to avoid the sensors overload. Nevertheless, in some cases, the signals were overloaded. In the case of Tinajas Bridge, Etna stations of Kinemetrics were used with internal triaxial accelerometers with a nominal sensitivity of $1.25\,\mathrm{V/g}$. Here, the sampling frequency was $f_s = 250\,\mathrm{Hz}$.

The modal parameters of the bridges were identified from ambient vibration data by the

(a)

(b)

Figure 1: (a) Location of the bridges in Spain and (b) experimental set-up.

stochastic subspace identification technique [4]. The ambient vibration response was acquired during the tests while the trains were not crossing the bridges. Data were decimated to carry out data analysis in the frequency range of interest ($0-30\,\mathrm{Hz}$). The signals were filtered applying two third-order Chebyshev filters with high-pass and low-pass frequencies of $1\,\mathrm{Hz}$ and $30\,\mathrm{Hz}$, respectively.

The dynamic characterisation of the soil was carried out by the seismic refraction and the Spectral Analysis of Surface Waves (SASW) tests. The seismic refraction test allowed the identification of the P-wave velocity (C_p) of the soil layers. The SASW test was used to determine the S-wave velocity (C_s), and the material damping ratio of the soil layers (β) was estimated by the half-power bandwidth method [5]. 100 hammer impacts were applied to a $50\,\mathrm{cm} \times 50\,\mathrm{cm} \times 8\,\mathrm{cm}$ aluminium foundation anchored to the soil surface (Figure 2). The instrumented hammer included a PCB 086D50 force sensor. The vertical free field response was recorded by means of accelerometers anchored to the soil surface every $2\,\mathrm{m}$ (from $2\,\mathrm{m}$ to $72\,\mathrm{m}$). Steel stakes of cruciform section and $30\,\mathrm{cm}$ of length were driven into the ground surface and the accelerometers were screwed to these stakes. After each impact, a time signal of 16348 samples ($4\,\mathrm{s}$) was stored. The force channel was used as a trigger, a pre-trigger of $1\,\mathrm{s}$, and a post-trigger of $3\,\mathrm{s}$. In this case, the signals were decimated (order 4), filtered with a third-order

Chebyshev filter with a high-pass frequency of $1\,\mathrm{Hz}$ and a low-pass frequency of $100\,\mathrm{Hz}$.

Figure 2: Soil test set-up close to one of the bridges under study.

3 Railway Bridges

In what follows, the specificities of the experimental set-ups and the experimental measurements recorded in Old Guadiana, Jabalón HSL, Jabalón, Algodor and Tinajas bridges are outlined.

During the recordings, several RENFE trains (S100, S102, S104, S112, S120, S130, S449, S599, Altaria and freight trains) crossed the bridges. Figure 3 includes the axle schemes and coach distributions of series S100, S102, S104, S120 and Altaria trains. Also the axle distances d and axle loads P are provided. More information in this regard can be found in Reference [6].

3.1 Old Guadiana Bridge

3.1.1 Description of the structure

This first bridge under study crosses Old Guadiana River in the conventional railway line Madrid-Alcázar de San Juan-Jaén, in the Alcázar de San Juan-Manzanares section (see Figure 4). It is a double-track concrete bridge composed by two identical simply-supported bays. The horizontal structure is formed by two structurally independent although adjacent decks, one for each track, sharing the ballast layer. Each deck is composed of a concrete slab resting on five pre-stressed concrete $0.75\,\mathrm{m} \times 0.3\,\mathrm{m}$ rectangular girders with no transverse stiffening elements (see Figure 5). The longitudinal girders rest on the two abutments and on a central pile support through neoprene bearings. Each deck accommodates a ballasted eccentric track with Iberian gauge ($1668\,\mathrm{mm}$), UIC60 rails and mono-block concrete sleepers separated $0.60\,\mathrm{m}$.

The vertical acceleration response was measured at 18 points of the lower flange lower horizontal face of the pre-stressed concrete girders (points $1-18$ in Figure 6). The accelerometers were attached to the girders using circular aluminium plates with $9\,\mathrm{cm}$ of diameter and $6\,\mathrm{mm}$ of thickness fixed with epoxy resin to the concrete surface (see Figure 1.(b)) which was previously treated for proper adherence. The response at points of the two decks in both spans was recorded.

Renfe Class 100

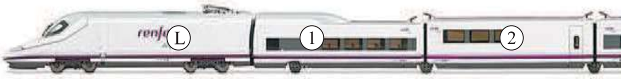

Renfe Class 102

Renfe Class 104

Renfe Class 120

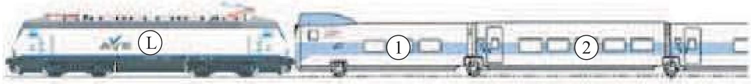

Renfe Altaria

Train	Renfe S100		Renfe S102		Renfe S104		Renfe S120		Altaria-13	
	d [m]	***P*** [kN]	***d*** [m]	***P*** [kN]	***d*** [m]	***P*** [kN]	***d*** [m]	***P*** [kN]	***d*** [m]	***P*** [kN]
Axle 1	3.78	174	4.585	170	3.85	153	4.11	153		225
Axle 2	3	174	2.65	170	2.7	153	2.8	153	3	225
Axle 3	11	174	8.35	170	16.3	153	16.2	150	7.5	225
Axle 4	3	174	2.65	170	2.7	153	2.8	150	3	225
Axle 5	3.1	140	5.735	156	4.2	153	3.613	161	6.74	70
Axle 6	3	140	10.52	161	2.7	153	2.8	161	9.84	140
Axle 7	15.595	160	13.14	170	16.3	153	16.2	162	13.14	140
Axle 8	3	160	13.14	167	2.7	153	2.8	162	13.14	140
Axle 9	15.7	160	13.14	161	4.2	153	3.613	155	13.14	140
Axle 10	3	160	13.14	159	2.7	153	2.8	155	13.14	140
Axle 11	15.7	160	13.14	166	16.3	153	16.2	159	13.14	140
Axle 12	3	160	13.14	166	2.7	153	2.8	159	13.14	140
Axle 13	15.7	172	13.14	170	4.2	153	3.613	158	13.14	140
Axle 14	3	172	13.14	166	2.7	153	2.8	158	13.14	140
Axle 15	15.7	160	13.14	170	16.3	153	16.2	157	13.14	140
Axle 16	3	160	13.14	166	2.7	153	2.8	157	13.14	140
Axle 17	15.7	160	10.52	163					13.14	140
Axle 18	3	160	5.735	170					9.84	70
Axle 19	15.7	160	2.65	170						
Axle 20	3	160	8.35	170						
Axle 21	15.595	140	2.65	170						
Axle 22	3	140								
Axle 23	3.1	174								
Axle 24	3	174								
Axle 25	11	174								
Axle 26	3	174								

Figure 3: Trains coach distribution and axle distances.

3.1.2 Modal parameters identification

Ten modes with natural frequencies below $30\,\text{Hz}$ are identified from the ambient vibration recorded during $3600\,\text{s}$. In Figure 7 the first ten mode-shapes are represented.

In Table 1 the identified natural frequencies and the damping ratios from the ambient response are included for the first ten modes. In the fundamental mode the identified damping ratio reaches 2.3%, higher than the value prescribed by standards for design purposes for this particular length and bridge typology (1.5% as per [7]).

The bridge response under operational conditions strongly depends on structural damping. Obtaining a realistic value of modal damping representative of the bridge dynamic response

Figure 4: Old Guadiana Bridge (39°17'37.8"N 3°12'22.5"W).

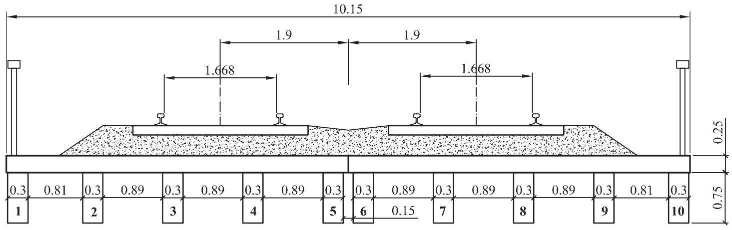

Figure 5: Old Guadiana Bridge deck cross section (Dimensions in [m]).

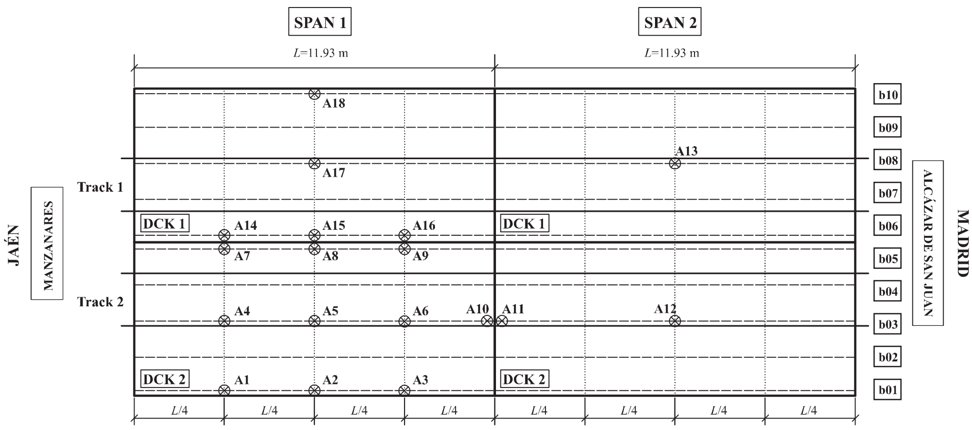

Figure 6: Location of the sensors at Old Guadiana Bridge.

under forced vibration is complicated, partially due to the dependency of this parameter with the amplitude of vibration. For this reason, modal damping has been also identified from the free vibration response recorded after the train passages indicated in section 3.1.4, using 10 s of free vibration. The modal damping ratios are extracted by the methodology presented by Kim et al. [8].

The damping ratio estimations are presented in Figure 8 and Table 1. The values of damping estimated from ambient vibration are represented with solid circles and compared to the values obtained from the train passages. The obtained results for the same vehicle crossing the bridge along the same track are consistent. As a general conclusion, it can be mentioned that the damping ratios from the train passages were considerably higher than those obtained from

Mode	f [Hz]	ξ_{AV} [%]
1	9.8	2.3
2	11.0	0.9
3	12.8	1.0
4	16.5	0.3
5	17.9	0.1
6	21.0	1.0
7	22.2	1.2
8	23.7	0.4
9	27.8	1.1
10	28.7	0.1

Mode	$\bar{\xi}_{TP}$ [%]	σ_{TP} [%]
1	2.9	0.6
2	2.5	0.5
3	1.5	0.3
4	1.9	0.1
5	1.7	0.1
6	1.3	0.2
7	1.4	0.2
8	1.2	0.1
9	1.2	0.2
10	1.0	0.2

Table 1: (left) Identified natural frequencies and damping ratios from ambient vibration and (right) mean and standard deviation of the identified damping ratios from free vibration after train passages in Old Guadiana Bridge.

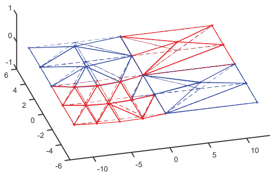

(a) Mode 1: $f_1 = 9.8\,\mathrm{Hz}$

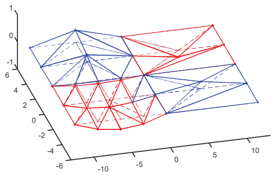

(b) Mode 2: $f_2 = 11.0\,\mathrm{Hz}$

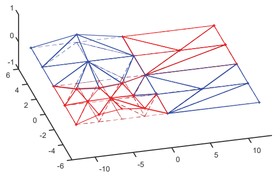

(c) Mode 3: $f_3 = 12.8\,\mathrm{Hz}$

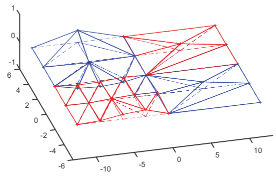

(d) Mode 4: $f_4 = 16.5\,\mathrm{Hz}$

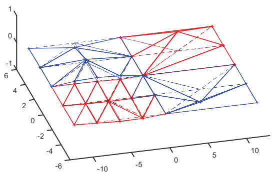

(e) Mode 5: $f_5 = 17.9\,\mathrm{Hz}$

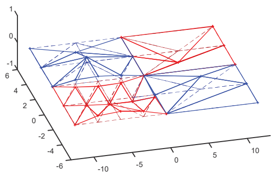

(f) Mode 6: $f_6 = 21.0\,\mathrm{Hz}$

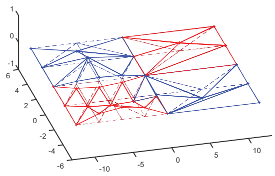

(g) Mode 7: $f_7 = 22.2\,\mathrm{Hz}$

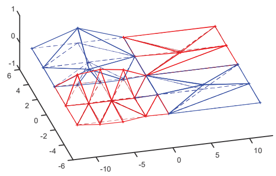

(h) Mode 8: $f_8 = 23.7\,\mathrm{Hz}$

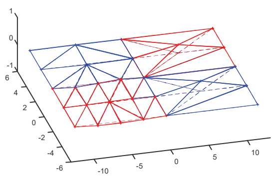

(i) Mode 9: $f_9 = 27.8\,\mathrm{Hz}$

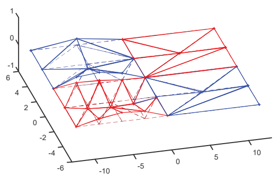

(j) Mode 10: $f_{10} = 28.7\,\mathrm{Hz}$

Figure 7: Identified mode shapes in Old Guadiana Bridge.

ambient vibration (factors of 1.3, 2.8 and 1.5 can be detected considering the mean value for all the trains in modes from 1 to 3). Notwithstanding the uncertainties, the estimations from the railway traffic were done under operational conditions of the bridge and can represent better the actual behaviour of the structure.

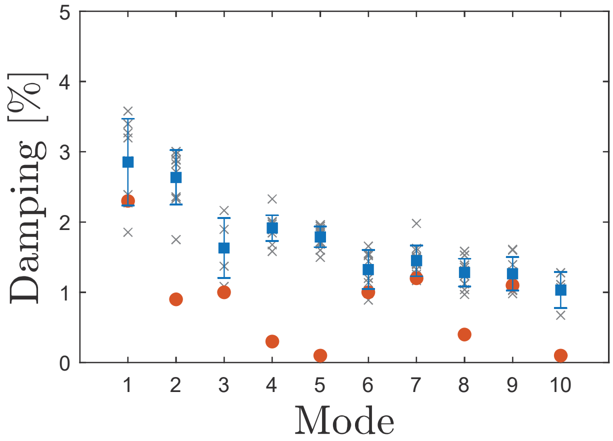

Figure 8: Old Guadiana bridge: estimated damping ratios from (red circle) ambient vibration and (grey crosses) train passages. The (blue square) mean value and (blue line) the mean value $\pm$ the standard deviation (σ) are also presented.

3.1.3 Soil properties identification

Following the procedure described in Section 2, the main dynamic properties of the soil are identified in the proximities of Old Guadiana Bridge. Figure 9 shows the resulting dispersion curve. The maxima in the spectrum are due to the Rayleigh waves. Table 2 shows the soil properties obtained from the resolution of the inverse problem using the elastodynamics toolbox (EDT) from Schevenels et al. [9].

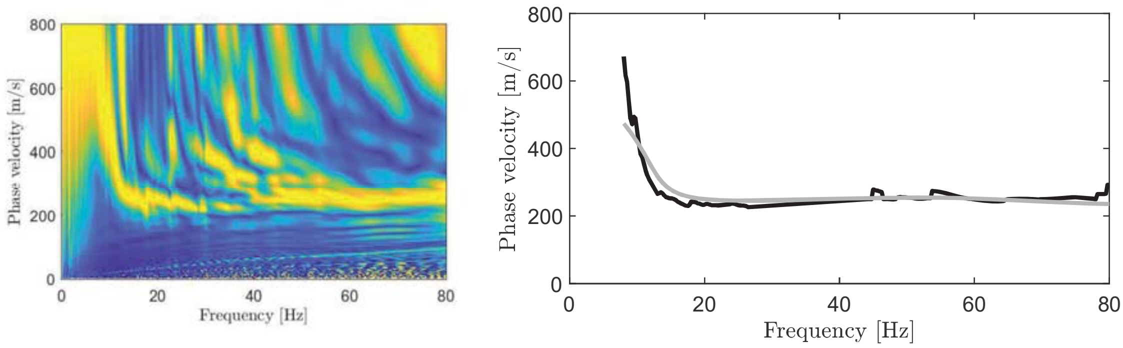

(a) (b)

Figure 9: Old Guadiana Bridge: (a) experimental dispersion curve and (b) solution of the inverse problem: experimental (black line) and numerical (grey line).

Layer	h [m]	C_p [m/s]	C_s [m/s]	ρ [kg/m^3]	β [-]
1	2	499	298	1900	0.08
2	4.5	350	207	1900	0.05
3	3.6	1300	719	1900	0.05
4	∞	500	250	1900	0.09

Table 2: Identified soil properties at Old Guadiana Bridge.

The soil presents two upper layers with a shear wave velocity lower than 300 m/s on a half-space with $C_s = 250$ m/s. The bridge supports at the abutments consist of spread footings. Therefore, in this case, SSI could affect to a certain extent the dynamic properties of the structure and its structural behaviour [10, 11].

3.1.4 Response due to train passages

The bridge response under thirteen circulations was recorded on May 6^{th} between 12:18 and 17:38 hours. In Table 3 the following information is included for each passage: train type, track number according to Figure 6, traffic direction, travelling speed, coaches scheme (L: locomotive, C: carriage) and average axle load P_k for the passenger coaches. Altaria trains, composed by a Talgo 252 locomotive and either 9 or 13 passenger coaches, are regular trains with a characteristic distance between shared axles of 13.14 m. S449 trains are articulated trains with distributed power, five coaches in total and a distance between shared bogies in the central carriages of 17.75 m. Trains S599 are conventional trains composed by two external power cars and a central carriage, and present a car length of approximately 25 m. Only one of the trains was a freight train with a conventional scheme as well. All passenger trains were commercial RENFE medium distance trains. Except for the second circulation, all the trains crossed the bridge at speeds in the interval $[140, 160]$ km/h.

Passage	Train	Track	Ride	Speed [km/h]	Scheme	$P_k/axle$ [kN]
1	Altaria-9	2	M-A	160	L-9C	140
2	S599	2	M-A	80	L-C-L//L-C-L	131
3	Altaria-13	2	M-A	160	L-13C	140
4	S449	1	A-M	160	L-3C-L	161
5	S449	1	A-M	160	L-3C-L	161
6	S449	2	M-A	160	L-3C-L	161
7	S599	1	A-M	143	L-3C-L	131
8	Altaria-13	1	A-M	157	L-13C	140
9	Altaria-9	1	A-M	155	L-9C	140
10	Freight train	1	A-M	-	L-13C	-
11	S449	2	M-A	160	L-3C-L	161
12	S449	1	A-M	160	L-3C-L	161
13	S449	2	M-A	160	L-3C-L	161

Table 3: Train passages recorded at Old Guadiana Bridge. M: Manzanares and A: Alcázar de San Juan.

In Figure 10 the acceleration response at two pair of sensors located at midspan of either span is represented in the frequency domain for train passages #1, #3, #5, #6, #9, #11, #12 and #13. One of the sensors is located under the loaded track and the other one under the unloaded track in all the cases. The maximum static load acting simultaneously on each of the spans, taking into account the span length, the particular axle loads, and the bogie and axle distances for the three types of trains is quite different: 140 kN for Altaria Talgo trains (one axle), 322 kN for S449 (two axles) and 524 kN for S599 trains (four axles). This may be the reason why many of the sensors were overloaded during train passages #2 and #7. In all the cases the response presents peaks associated to the excitation (i.e. ratio of train speed v to bogie and axle distances v/d_{bogie} and v/d_{axle}, respectively, and corresponding multiples) and to the bridge lowest natural frequencies. In the case of Altaria Talgo trains, the acceleration amplitude in the vicinity of the bridge fundamental frequency stands out considerably in comparison to the peaks associated to the excitation. This is not the case for the S449 or the S599 trains. This is partially related to the fact that the former trains with a characteristic distance of 13.14 m travel at a velocity close to the theoretical third resonant speed of the fundamental mode of the bridge: $v_{1,3} = 9.8 \times 13.14/3 \times 3.6 = 154$ km/h, in combination with the high number of passenger coaches. The maximum overall acceleration measured during the train passages for frequency contents below 30 Hz reaches 1.61 m/s^2, close to one half of the limit established by the Serviceability Limit State for traffic safety 3.5 m/s^2 for bridges with ballasted tracks [12]. This maximum takes place under Altaria train with 9 passenger coaches crossing the bridge along track 2 northbound (circulation #1). Similar amplitudes of the vertical acceleration are measured for the second circulation. Nevertheless, it should be said that the actual maximum acceleration most probably took place in an overloaded sensor and is higher than the previously mentioned value. In the plots included in Figure 10 the acceleration response in the sensor located in the unloaded deck is, in some cases, of the same order of magnitude than that measured in the loaded deck. For sensors 5 and 17 (centre of the decks) the response at the unloaded sensor is relevant at the fundamental frequency (first longitudinal bending mode); and for sensors 2 and 18 (external borders of the decks) the unloaded sensor response has also important contributions at other identified frequencies, indicating an important coupling between the two decks of the same span through the ballast layer. This issue was already detected under ambient vibration and seems to be also important under the circulation of trains, despite the much higher vibration amplitudes of the structure in this case. The coupling between the adjacent decks is analysed in more detail for the Altaria trains in what follows.

Figure 11 shows the bridge response at sensors 5, 17, 8 and 15 due to a Renfe Altaria train travelling along tracks 1 (red trace) and 2 (black trace) at $v = 160$ km/h and $v = 155$ km/h, respectively (circulations #1 and #9). Therefore, this figure shows the response of the two adjacent decks in the first span under the circulation of two identical trains travelling at very similar speeds in the two opposite directions. As mentioned before, the resonant speeds for the fundamental mode and third resonance is $v_{1,3} = 154$ km/h, very close to the actual speeds. The damping ratios for the first mode obtained from the free vibration response after the trains left the structure were in these cases 2.2% and 2.8%, respectively. The response measured at points 5 and 17 (Figure 6) presents a very high similarity when the trains cross the bridge along either of the two tracks (i.e. the unloaded and loaded sensor responses are very similar no matter what is the train direction). This shows that both decks dynamic responses are very similar and that the coupling effect is bidirectional. The contribution of mode 1 clearly prevails in all the sensors and that of the third mode (transverse bending mode) is clearly visible at points 8 and 15. Moreover, the characteristic vehicle frequency $v/d = 160/3.6/13.14 = 3.4$ Hz and its second harmonic can also be observed at the sensors installed at the loaded deck (and are almost imperceptible at the unloaded one). When the Altaria train crosses the bridge along track 2 induces a higher acceleration response in deck 2 (sensors 5 and 8), as expected. Nevertheless, the levels of the amplitudes measured at deck 1 (sensors 15 and 17) are considerable. The maximum acceleration amplitude in deck 1 is in that case approximately 45% of the highest acceleration measured in deck 2. Among the four selected sensors the one exhibiting the highest response is sensor 8, at the longitudinal edge of deck 2, in the loaded case, showing an important contribution of the fourth mode. Again, the coupled responses of the decks through the ballasted track are significant.

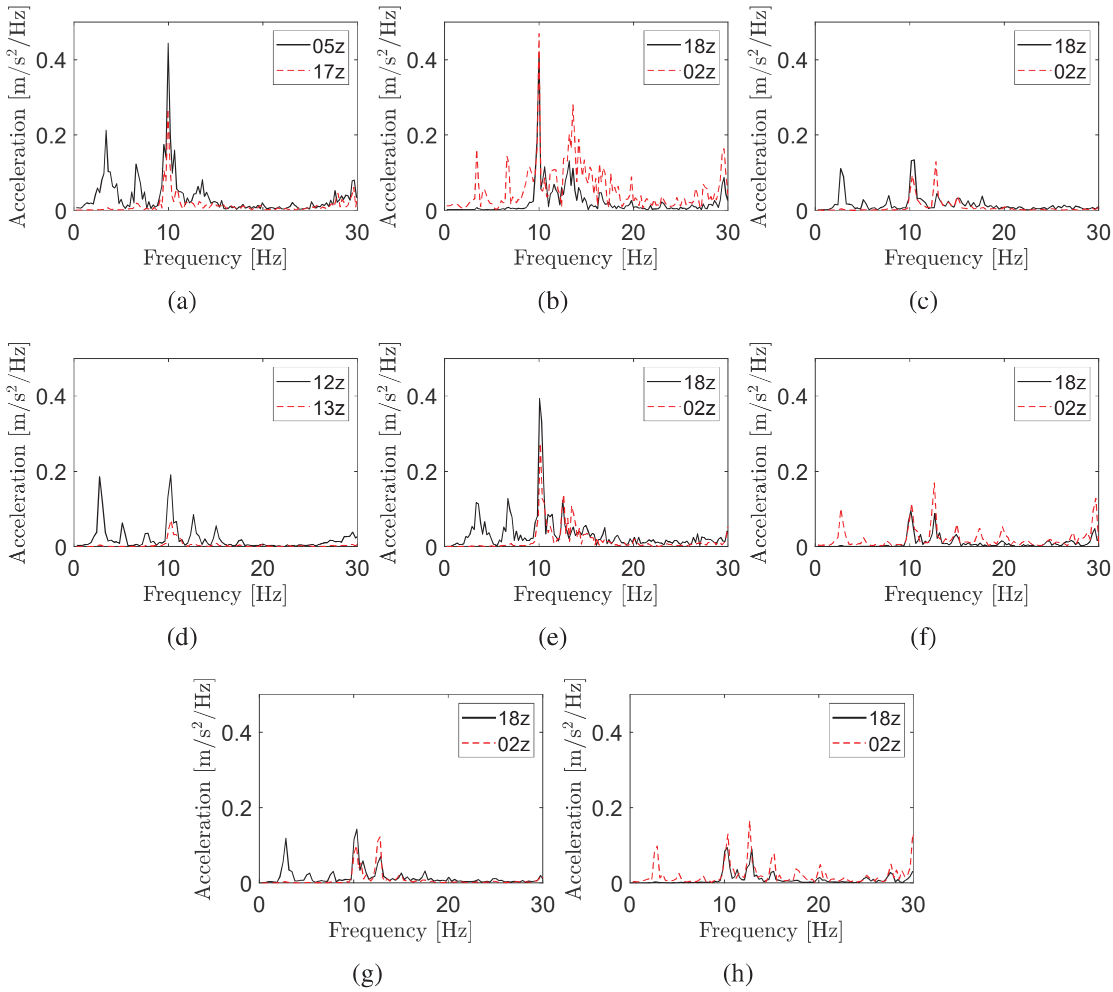

Figure 10: Old Guadiana Bridge: frequency content of the structural acceleration induced by train (a) #1, (b) #3, (c) #5, (d) #6, (e) #9, (f) #11, (g) #12 and (h) #13

3.2 Jabalón HSL Bridge

3.2.1 Description of the structure and properties identification

Jabalón HSL Bridge (Figure 12), is a railway bridge composed by three identical S-S bays of 24.9 m equal spans. The structure crosses Jabalón River with a $134°$ skew angle. Each deck consists of a cast-in-situ concrete slab with dimensions 11.6 m $\times$ 0.3 m (wide $\times$ thickness). The slab rests over five prestressed concrete I girders with a height of 2.05 m separated 2.625 m (see Figure 13). The girders lean on the supports through laminated rubber bearings. The slab carries two ballasted tracks with UIC gauge (1435 mm), UIC60 rails and mono-block concrete sleepers every 0.60 m. The substructure consists of two outer reinforced concrete abutments and two inner wall piers. Figure 14 shows the measurement points, all of them located at span 1. Unfortunately, it was only possible to record the response of the first span due to the piers height and the river flow.

Table 4 presents the identified modal parameters of the structure.

Table 5 presents the identified dynamic soil properties. The experimental procedure described in section 3.1.3 is reproduced at this bridge site. The soil in the surroundings of Jabalón HSL bridge is composed of an upper layer of limestone of approximately 2 m with a shear wave

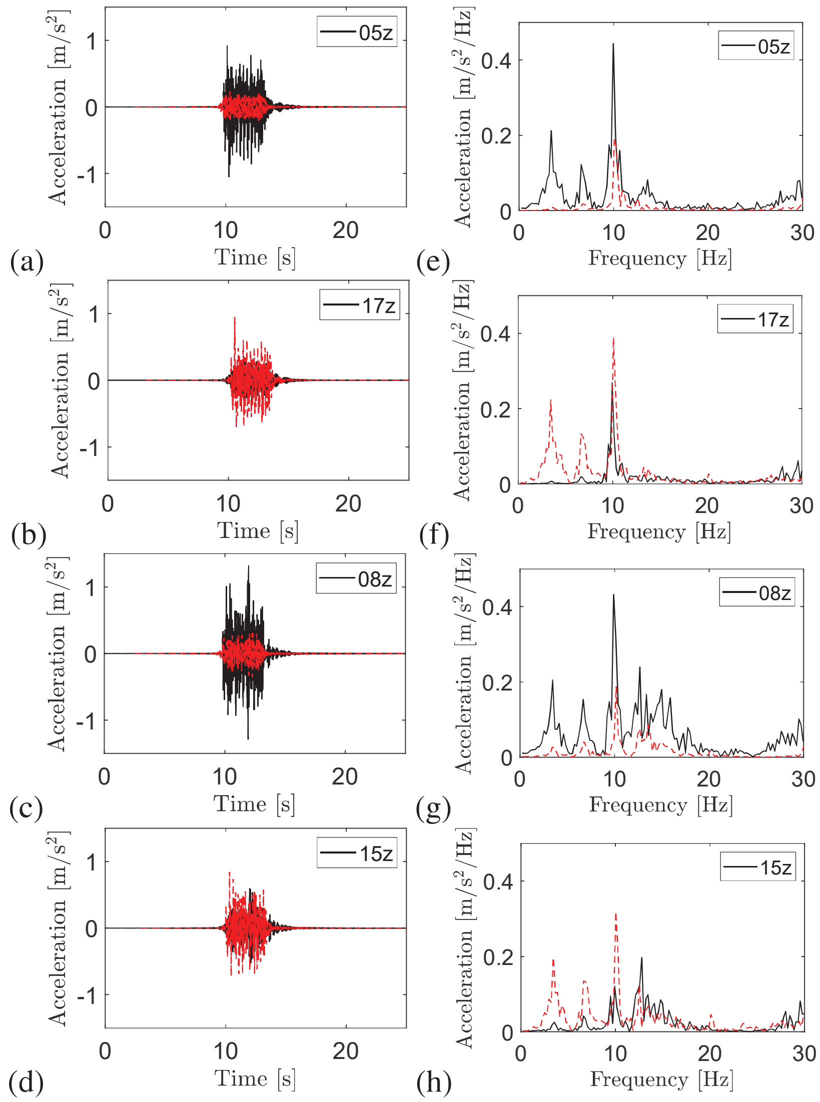

Figure 11: Old Guadiana Bridge: (a-d) time history and (e-h) frequency content of the acceleration at points 5, 17, 8 and 15 induced by Renfe Altaria train with 9 coaches (black line) at v = 160 km/h circulating on track 2 and (red line) at v = 155 km/h circulating on track 1.

Figure 12: HSL bridge over Jabalón River (38°53'51.3"N 3°57'53.0"W).

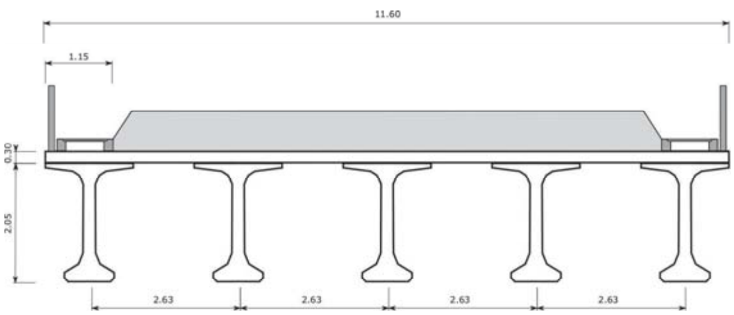

Figure 13: Jabalón HSL deck cross section (Dimensions in [m]).

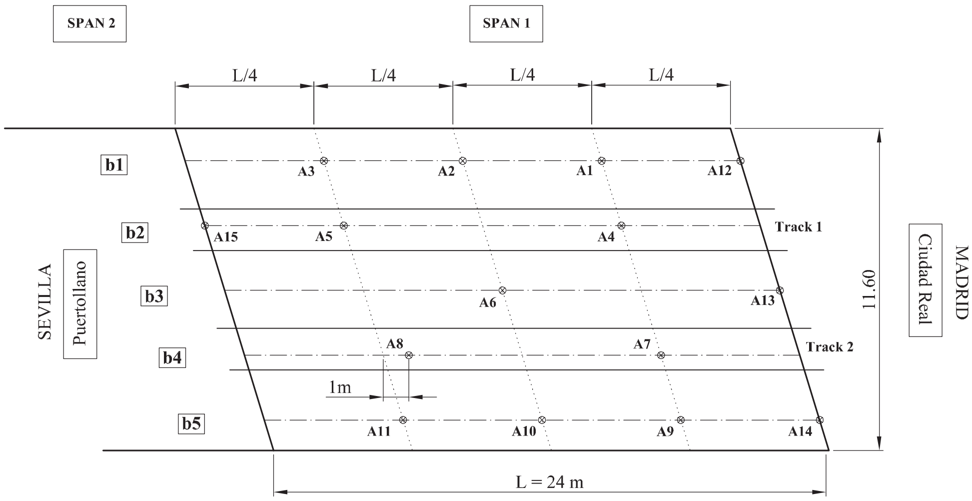

Figure 14: Location of the sensors on Jabalón HSL Bridge.

Mode	f [Hz]	ξ_{AV} [%]
1	6.3	3.2
2	7.2	1.6
3	9.3	0.7
4	14.8	0.6
5	24.0	1.2
6	24.5	0.8

Mode	$\overline{\xi}_{TP}$ [%]	σ_{TP} [%]
1	3.5	0.9
2	3.3	0.8
3	2.4	0.7
4	2.0	0.2
5	1.1	0.1
6	1.2	0.2

Table 4: (left) Identified natural frequencies and damping ratios from ambient vibration and (right) mean and standard deviation (σ) of the identified damping ratios from train-induced vibrations of Jabalón HSL Bridge.

velocity of $C_s = 321$ m/s, a layer of clay gravel of approximately 2 m and $C_s = 176$ m/s on a sand-clay halfspace with $C_s = 225$ m/s. The profile from the SASW test is consistent with that provided by a geotechnical analysis performed at the site prior to the bridge construction [13].

3.2.2 Response due to train passages

Table 6 summarizes the train passages recorded at Jabalón HSL Bridge. The dynamic response of the bridge under the circulation of 20 passenger trains was recorded on May 8^{th} 2019

Layer	h [m]	C_p [m/s]	C_s [m/s]	ρ [kg/m^3]	β [-]
1	2	800	321	2000	0.1
2	2	715	176	2000	0.1
3	∞	500	225	2000	0.1

Table 5: Identified soil properties at Jabalón Bridge.

between 11.52 and 15.24 hours. All the trains that travelled over the bridge in both directions were RENFE High-Speed services. In particular articulated S100 trains, regular S102, S112 and S130 trains, and conventional S104 trains crossed the bridge in single and duplex configurations. The identified travelling velocities are comprised between 236 and 290 km/h and are included in Table 6 along with the trains schemes and average axle loads of the passenger coaches.

The trains inducing the lowest dynamic response on Jabalón HSL bridge are S104 trains. These trains are composed by only two passenger coaches and their maximum speed is 250 km/h. The overall maximum acceleration reaches 1.8 m/s^2 (calculated after the signal is filtered under 30 Hz), and happens for the ninth circulation (S102 duplex at 265 km/h). A similar maximum level of the acceleration is obtained for circulations #4 and #12 for a similar and for the same train. S102 trains are regular Talgo trains with a short characteristic distance (13.14 m) and a high number of axles. Therefore this trains are prone to excite the participation of low frequency modes of the bridge. Again, one should be cautious with this value as some of the sensors overloaded and are not considered in the analysis. Sensors that particularly experienced overload are those close to the supports of the deck under the loaded track (13 and 15 when the trains travel along track 1, and 13 and 14 when they travel along track 2). A non symmetric dynamic behaviour is detected when comparing the responses between accelerometers 10 and 2, which may be related to the deck obliquity. In all the cases the response measured close to the abutments and to the intermediate pile are considerably lower in terms of accelerations than at the intermediate sections.

Figures 15, 16 and 17 compare the bridge response at four sensors under the circulation of three trains Renfe S104, Renfe S102 and Renfe S100 crossing the bridge a two similar (yet non-resonant) speeds. The first figure corresponds to train S104 travelling along track 1 southbound. The response at the sensors close to the loaded track (accelerometers 1 and 2) exhibits contributions in the frequencies v/d_i and corresponding harmonics, being d_i the characteristic length or distance between axles and between bogies of the trains. This train, in particular, does not excite the bridge natural frequencies to a big extent compared to S102 or S100, which are composed by a much higher number of passenger coaches. The responses for two travelling speeds are superimposed: 249 and 255 km/h. The responses are almost identical despite the small difference in the speeds. It should be said that the second and third theoretical resonant speeds for the fundamental mode associated to the coaches lengths are 196 and 294 km/h, far from the actual velocities. For this reason the response is not very sensitive to this parameter.

3.3 Algodor Bridge

The third bridge under study, Algodor Bridge, belongs to the Madrid-Sevilla High-Speed railway line as well. It is a railway bridge composed by three S-S bays with 10.25 m, 10.00 m and 10.25 m spans (distance between centres of neoprene bearings). The bridge crosses Algodor river with a skew angle of $114.3°$ (Figure 18). Algodor Bridge presents a filler beam deck,

Passage	Train	Track	Ride	Speed [km/h]	Scheme	$P_k/axle$ [kN]
1	S102	1	M-C	290	L-12C-L	165
2	S102	2	C-M	266	L-12C-L	165
3	S104	2	C-M	251	L-2C-L	153
4	S112-Duplex	1	M-C	267	L-12C-L//L-12C-L	172
5	S102	1	M-C	240	L-12C-L	165
6	S102-Duplex	2	C-M	263	L-12C-L//L-12C-L	165
7	S100	1	M-C	290	L-8C-L	156
8	S112	1	M-C	269	L-12C-L	172
9	S102-Duplex	2	C-M	265	L-12C-L//L-12C-L	165
10	S130	1	M-C	236	L-11C-L	165
11	S102	2	C-M	274	L-12C-L	165
12	S102-Duplex	1	M-C	267	L-12C-L//L-12C-L	165
13	S130	2	C-M	237	L-11C-L	165
14	S104	1	M-C	249	L-2C-L	153
15	S100	2	C-M	262	L-8C-L	156
16	S130	1	M-C	236	L-11C-L	165
17	S100	1	M-C	290	L-8C-L	156
18	S102	2	C-M	273	L-12C-L	165
19	S104	1	M-C	255	L-2C-L	153
20	S104	2	C-M	236	L-2C-L	153

Table 6: Train passages recorded at Jabalón HSL Bridge. M: Madrid and C: Ciudad Real.

composed by a 0.65 m thick and 11.6 m wide concrete slab longitudinally reinforced with 20 inverted T pre-stressed concrete girders enclosed within the depth of the slab and with the required steel rebars for transverse reinforcement (see Figure 19). The girders lean on the supports through laminated rubber bearings. The slab carries two ballasted tracks with UIC gauge (1435 mm), UIC60 rails and mono-block concrete sleepers every 0.60 m, and with an equal eccentricity of 2.15 m measured from its longitudinal axis. The bridge deck is supported on reinforced concrete abutments in its outermost sections and the inner sections of both bays lean on a 0.6 m thick and 12.3 m wide concrete pier. Figure 20 shows the measurement points. In this case, two of the three spans were monitored.

Five modes were identified from the ambient vibration response with frequencies up to 30 Hz. Table 7 and Figures 21 and 22 show the identified modal parameters. The first two modes correspond to the first longitudinal bending mode of each span vibrating out of phase and in phase, respectively. In modes 3 and 4 the deck deforms under torsion: in the former each span deforms independently and, in the latter, the torsional deformations of both spans are coupled. The last mode corresponds to the transverse bending deformation of one the spans. Modal damping is again identified both from ambient vibration and from the free vibration after the train passages. It should be mentioned in this case that modes 1 and 2, and modes 3 and 4 present very similar natural frequencies, which could bias the estimation of this parameter [8]. The identified damping for the fundamental mode from the train passages is 2.1%, higher than the ambient vibration estimation (1.5%) and than the value recommended by Eurocode (1.7%).

Table 8 shows the dynamic soil properties. The soil in the surroundings of Algodor Bridge is composed of an upper layer of gravel of approximately 2 m with $C_s = 314$ m/s on a clay on

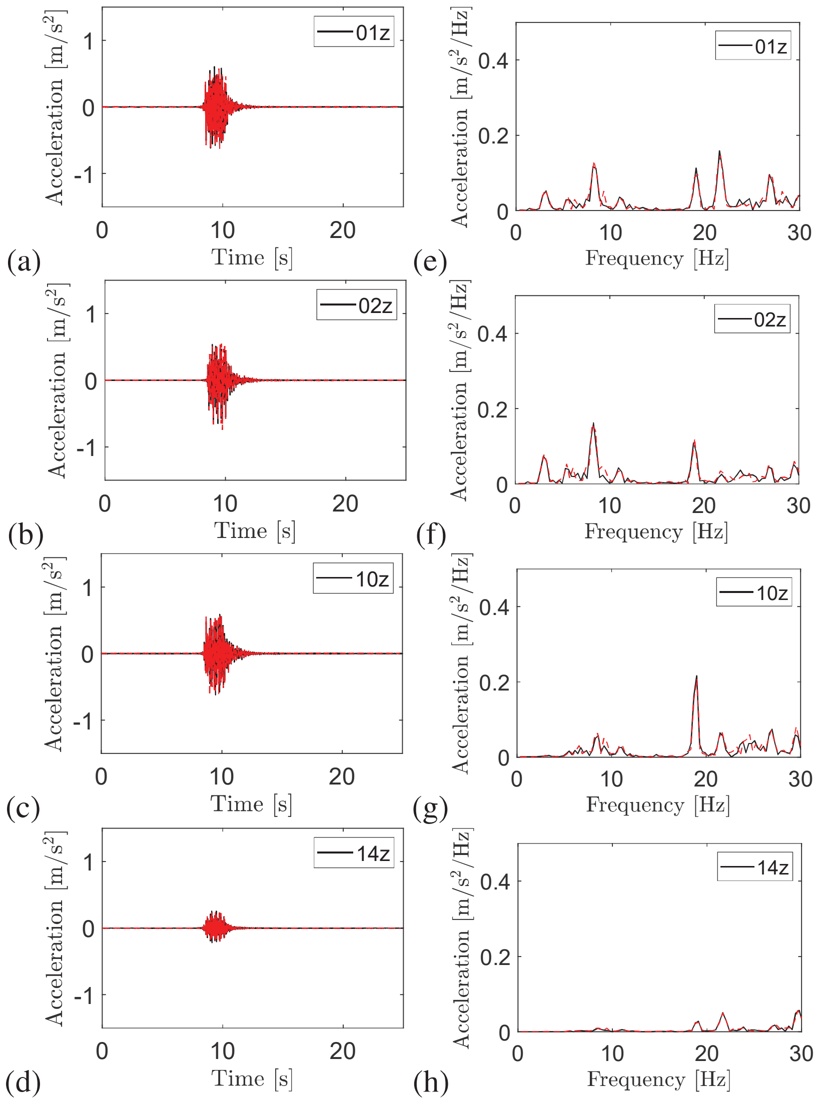

Figure 15: Jabalón HSL Bridge: (a-d) time history and (e-h) frequency content of the acceleration at points 1, 2, 10 and 14 induced by Renfe S104 train circulating on track 1 at (black line) $v = 249$ km/h and (red line) $v = 255$ km/h.

a slate halfspace with $C_s = 800$ m/s. The high identified value of the P-wave velocity indicates that the soil is saturated. The profile is consistent with that provided by a geotechnical analysis performed at the site prior to the bridge construction [14].

Mode	f [Hz]	ξ [%]
1	11.6	1.5
2	11.7	2.9
3	13.7	1.0
4	13.9	0.6
5	19.6	0.9

Mode	$\bar{\xi}_{TP}$ [%]	σ_{TP} [%]
1	2.1	0.4
2	1.9	0.4
3	1.8	0.5
4	1.8	0.6
5	1.1	0.2

Table 7: (left) Identified natural frequencies and damping ratios from ambient vibration and (right) mean and standard deviation (σ) of the identified damping ratios from train-induced vibrations in Algodor Bridge.

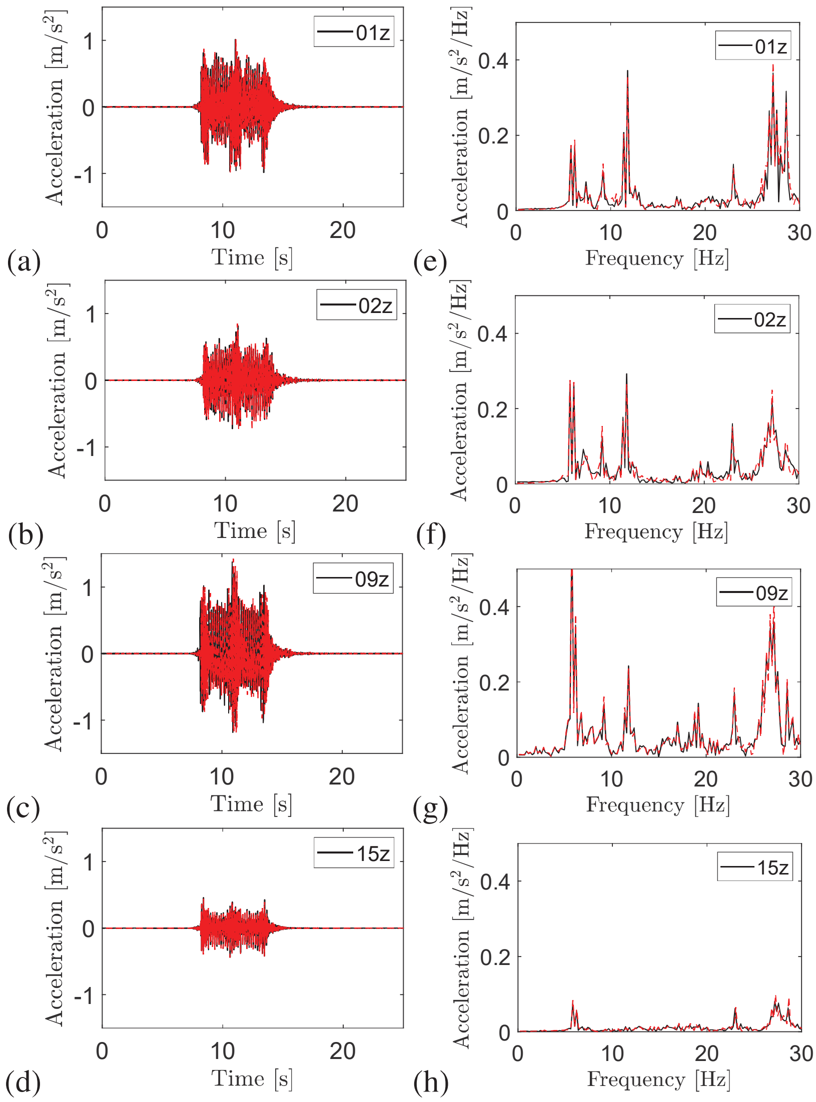

Figure 16: Jabalón HSL Bridge: (a-d) time history and (e-h) frequency content of the acceleration at points 1, 2, 9 and 15 induced by Renfe S102 duplex train circulating on track 2 at (black line) $v = 263$ km/h and (red line) $v = 265$ km/h.

Layer	h [m]	C_p [m/s]	C_s [m/s]	ρ [kg/m^3]	β [-]
1	2	554	314	2000	0.09
2	∞	1600	800	2000	0.07

Table 8: Identified soil properties at Algodor Bridge.

3.3.1 Response due to train passages

On May 5^{th} 2019 the response of Algodor Bridge under the circulation of 13 passenger trains was recorded. The particular trains were Renfe S102, S130 and S120, in single and duplex configurations, and Renfe S100. S102 and S130 are regular trains, S120 is a conventional train and S100 is articulated. Table 9 presents information in relation with these train passages. The travelling speeds were comprised between 228 and 307 km/h. The overall maximum acceleration measured was 2.96 m/s^2 under passages #2 and #3 of the S102 train at 304 km/h. This value was measured at accelerometer 1 (central span, central section border girder closest to the

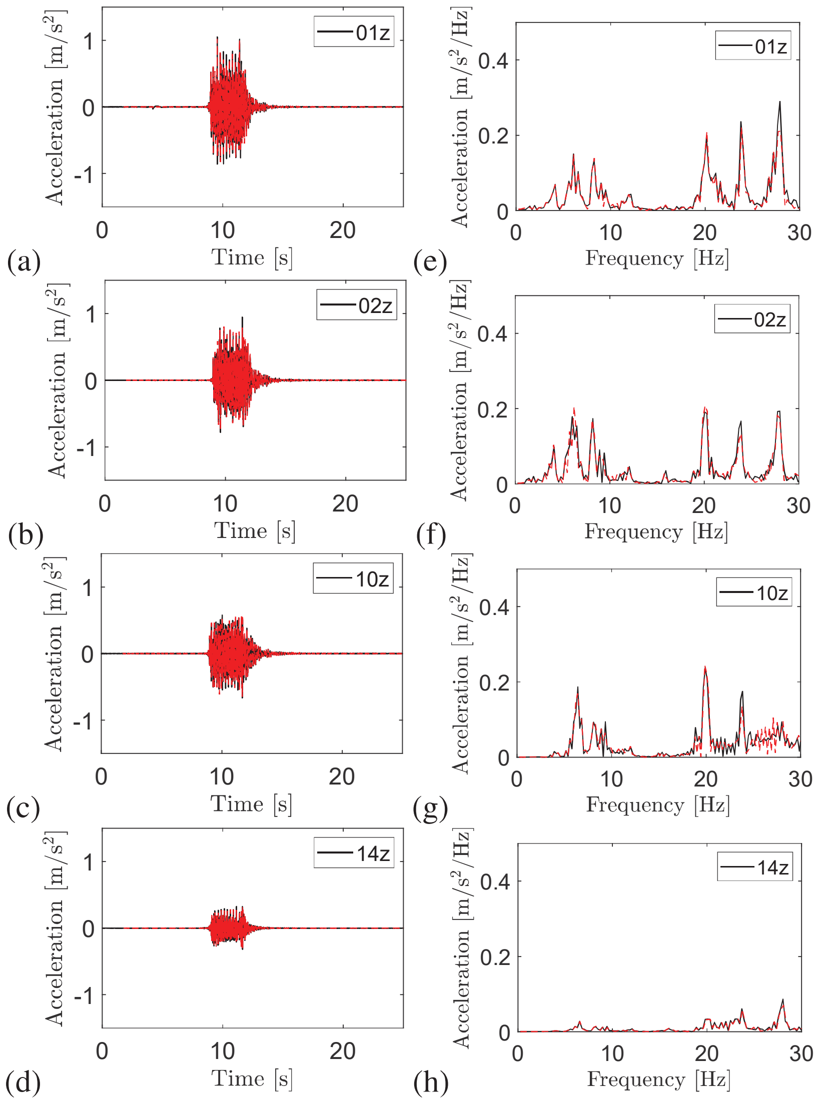

Figure 17: Jabalón HSL Bridge: (a-d) time history and (e-h) frequency content of the acceleration at points 1, 2, 10 and 14 induced by Renfe S100 train circulating on track 1 at (black line) $v = 290\,\mathrm{km/h}$ and (red line) $v = 290\,\mathrm{km/h}$.

Figure 18: Bridge over Algodor River (39°31’55.5”N 3°49’25.3”W).

loaded track). Some sensors were overloaded in some cases. In particular accelerometer 4, in

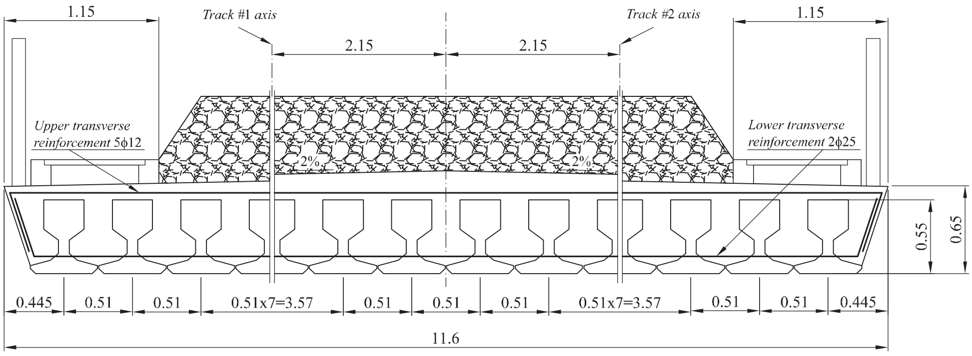

Figure 19: Algodor Bridge deck cross section (Dimensions in [m]).

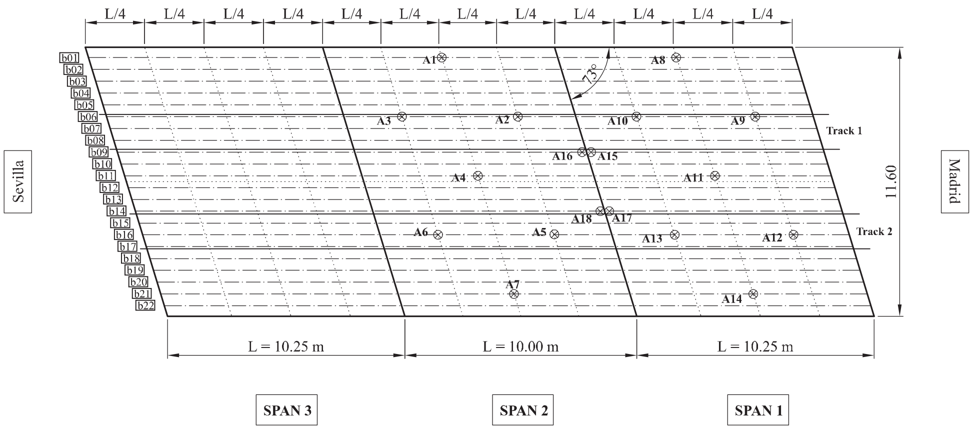

Figure 20: Location of the sensors on Algodor Bridge.

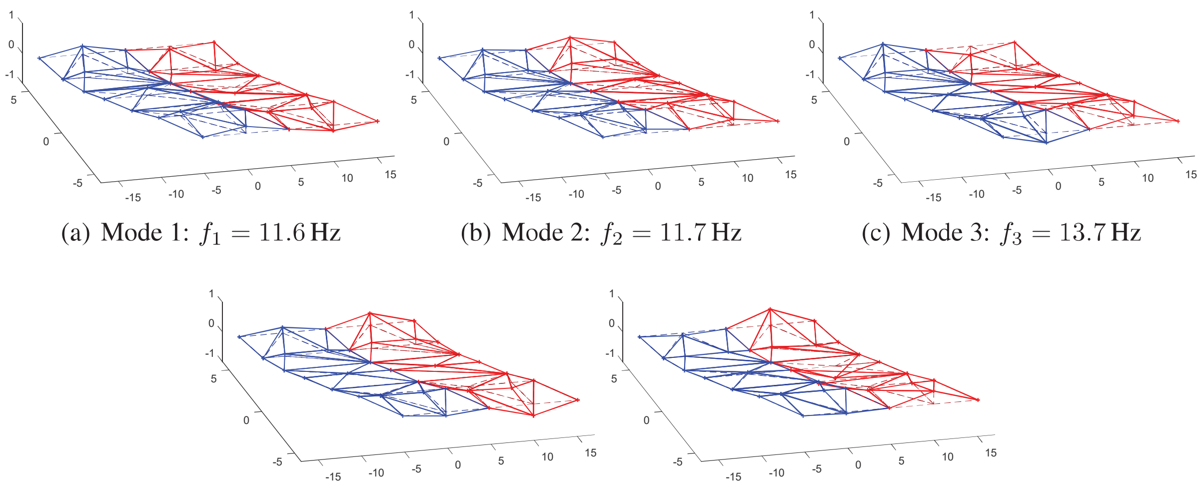

(a) Mode 1: $f_1 = 11.6\,\text{Hz}$ (b) Mode 2: $f_2 = 11.7\,\text{Hz}$ (c) Mode 3: $f_3 = 13.7\,\text{Hz}$

(d) Mode 4: $f_4 = 13.9\,\text{Hz}$ (e) Mode 5: $f_5 = 19.6\,\text{Hz}$

Figure 21: Identified mode shapes of Algodor Bridge: (red) span 1 and (blue) span 2.

the very centre of the second span, was overloaded under most of the circulations. Therefore, the maximum acceleration of the deck could be somewhat higher than the referred value.

Figure 23 shows the structural response induced by the fourth and ninth trains passages.

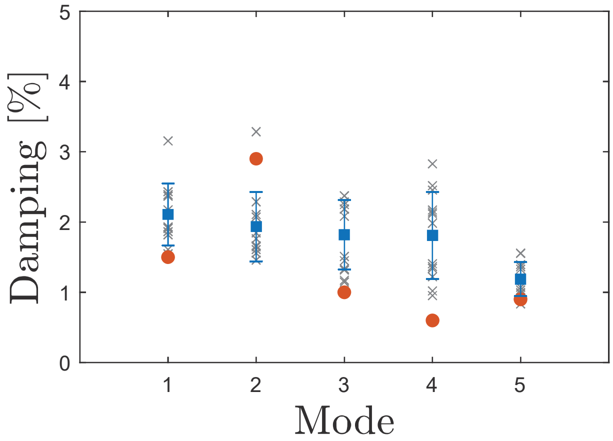

Figure 22: Algodor bridge: estimated damping ratios from (red circle) ambient vibration and (grey crosses) train passages. The (blue square) mean value and (blue line) the mean value $\pm$ the standard deviation (σ) are also presented.

These correspond to the circulation of two Renfe S102 trains travelling at $v = 304$ km/h along track 1 (black trace) and at $v = 306$ km/h along track 2 (red trace). The responses are compared at sensors 1 and 7 (mid section of the central span) and 8 and 11 (mid section of first span). The contribution of torsion modes (with frequencies close to 14 Hz) and transverse bending mode (with frequency close to 20 Hz) are the most relevant regardless of the train direction. In each span the decks of Algodor Bridge present very similar length and width dimensions. Also, the flexural and torsional stiffnesses are uniformly distributed due to the filler-beam typology of the deck. This justifies the plate-type dynamic response that this bridge in particular exhibits. The S102 trains velocities are far from any resonant condition of the longitudinal bending and torsion modes ($v_{1,2} = 274.4$ and $v_{3,2} = 324$ km/h for $f_1 = 11.6$ and $f_3 = 13.7$ Hz, respectively) but the third resonant frequency of the fifth mode (transverse bending mode) is induced by this train travelling at $v_{3,3} = 13.14 \times 19.6 \times 3.6/3 = 309$ km/h. This may be the reason why an important amplification happens close to 20 Hz.

Passage	Train	Track	Ride	Speed [km/h]	Scheme	P_k/axle [kN]
1	S102-Duplex	1	M-C	298	L-12C-L//L-12C-L	165
2	S130-Duplex	2	C-M	228	L-11C-L//L-11C-L	165
3	S102	1	M-C	304	L-12C-L	165
4	S102	1	M-C	304	L-12C-L	165
5	S102-Duplex	2	C-M	252	L-12C-L//L-12C-L	165
6	S120	2	C-M	250	L-2C-L	160
7	S102-Duplex	2	C-M	260	L-12C-L//L-12C-L	165
8	S120-Duplex	1	M-C	238	L-2C-L//L-2C-L	160
9	S102	2	C-M	306	L-12C-L	165
10	S130-Duplex	1	M-C	237	L-11C-L//L-11C-L	165
11	S130	2	C-M	229	L-11C-L	165
12	S102	1	M-C	298	L-12C-L	165
13	S100	2	C-M	307	L-8C-L	156

Table 9: Train passages recorded at Algodor Bridge. M: Madrid and C: Ciudad Real.

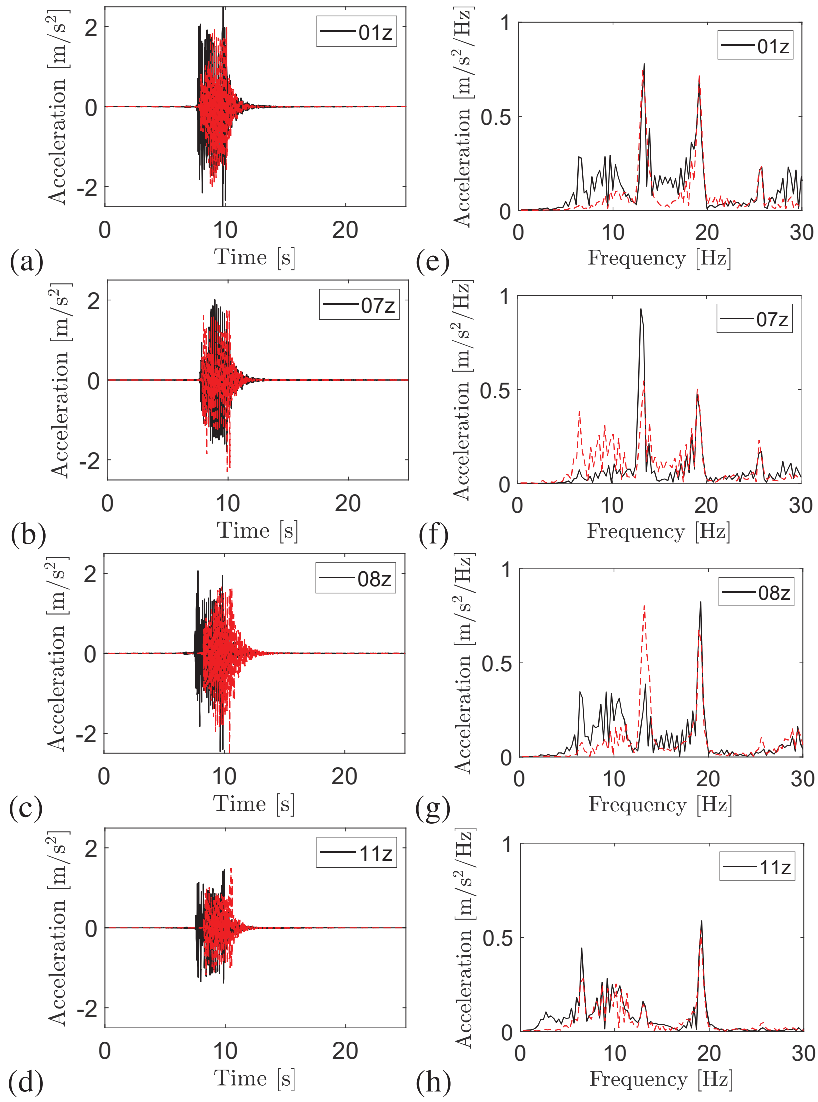

Figure 23: Algodor Bridge: (a-d) time history and (e-h) frequency content of the acceleration at points 1, 7, 8 and 11 induced by Renfe S102 train circulating (black line) on track 1 at $v = 304$ km/h and (red line) on track 2 at $v = 306$ km/h.

3.4 Jabalón Bridge

Jabalón Bridge (Figure 24), is a steel truss railway bridge composed by three S-S bays of 25 m of span. This bridge also crosses Jabalón river but it belongs to the conventional railway line Alcázar de San Juan-Ciudad Real-Badajoz. In this section nowadays the traffic is very limited and most of the circulations are freight trains and maintenance vehicles. Jabalón and Jabalón HSL are only 200 m apart and one set of tests were performed in the area in order to identify the soil properties (see section 12). Jabalón Bridge carries only one ballastless track (Figure 25 left) with Iberian gauge, UIC60 rails and wooden sleepers. Due to the absence of ballast and direct contact between the rail and the steel structure, unfortunately, several accelerometers were unstuck due to the high level of vibrations induced by the train passages. In what follows a few remarks are included in relation to the behaviour of this particular structure but the information available is much less than in the previous cases.

Figure 26 shows the measurement points. The accelerometers were glued directly at the truss connections in different orientations (see Figure 25 right). Three modes were clearly identified from ambient vibration (see Table ??). In increasing frequency order these modes correspond to first lateral bending, first longitudinal bending and first torsion modes. In this case, only damping values identified from ambient vibration are available. The fundamental mode exhibits very low damping, typical in steel structures but the values obtained for the second and third modes are comparable to the values identified in previous bridges. The modal damping value proposed by Eurocode [7] for this steel bridge is 0.5%.

Figure 24: Bridge over Jabalón River (38°53’51.2”N 3°57’44.7”W).

Figure 25: (left) Track in the Bridge over Jabalón River and (right) accelerometer at the truss connection.

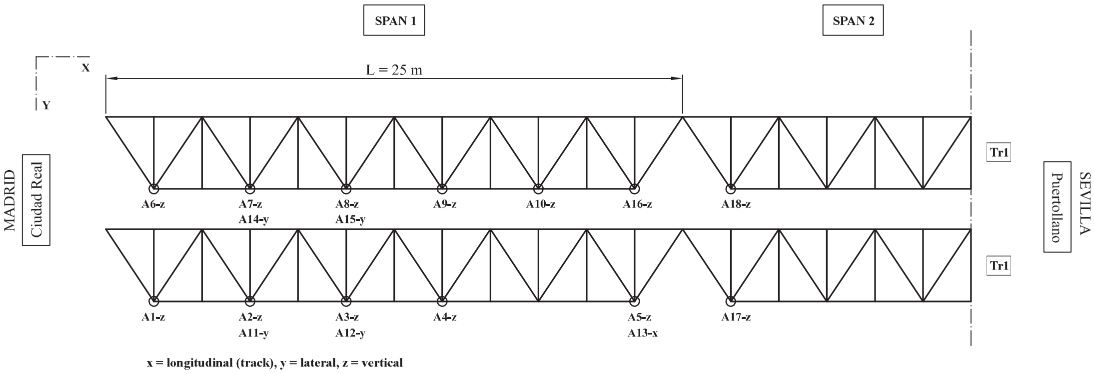

Figure 26: Location of the sensors on Jabalón Bridge.

3.5 Tinajas Bridge

The bridge over the Tinajas Stream (Figure 27) is a three-span continuous bridge with span lengths of 25 m, 35 m and 25 m. At the moment of the experimental campaign this bridge was under construction. It belongs to the conventional railway line between Bobadilla and Algeciras. The bridge presents a steel-concrete composite section formed by two main steel I beams and an upper concrete slab. The slab is 8.6 m wide allowing the installation of a single-track with Iberian gauge, UIC60 rails and mono-block concrete sleepers every 0.60 m (Figure 28). The height of the I beams is 1.8 m. The concrete slab presents variable thickness from 0.20 m to 0.38 m. Close to the intermediate supports the section is completed with a lower concrete slab with a thickness of 0.20 m. The two main steel beams are reinforced with sheets of variable thickness in the lower flange ($30 - 60$ mm) and web ($15 - 20 - 25$ mm), and with steel plates of constant thickness (25 mm) in the upper flange. The beams are braced every 5 m with H-shaped transverse frames. The deck is supported on two abutments at the outermost sections and on two concrete piles at the inner supports, all of them with micropiles. The deck rests on eight POT bearings positioned under each beam longitudinal axis at the piles and abutments. Transversely the deck movement is restricted by seismic supports installed at each pile and abutment. The longitudinal moving support is materialized at one of the abutments. The rectangular concrete piles have a cross section of $4.50\,\text{m} \times 1.50\,\text{m}$ and heights of 16.60 m and 16.01 m, respectively.

Figure 27: Bridge over Tinajas River (37°01'41.0"N 4°45'26.6"W).

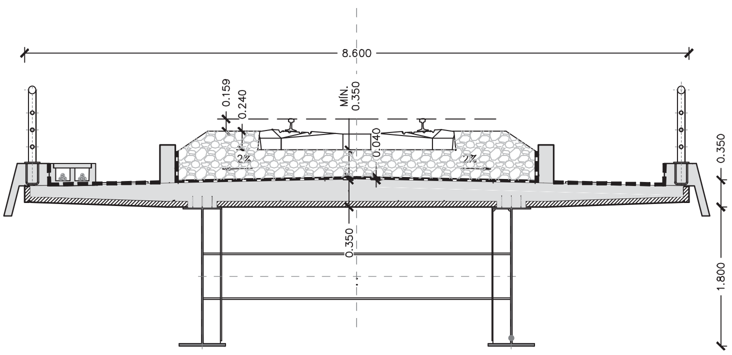

Figure 28: Tinajas Bridge deck cross section (Dimensions in [m]).

The ambient response of the bridge deck was measured at 18 points using triaxial accelerometers (Figure 29). Table 10 and Figure 30 present the identified modal parameters. In the first five mode shapes the deck deforms under lateral bending (mode 1), longitudinal bending (modes 2 and 5) and torsion (modes 3 and 4). Very low damping values, in the range $[0.4-0.7]\%$, were identified for the five modes in ambient vibration, close to the Eurocode recommendation of 0.5% for spans longer than $20\,\mathrm{m}$ in the case of steel-concrete composite bridges. Modal parameters were not identified in free vibration as the bridge was not operational during the measurements. In this case, soil tests were not performed.

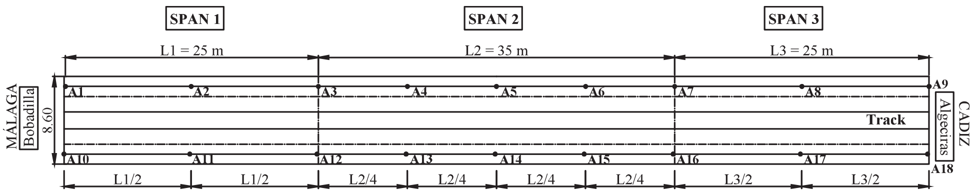

Figure 29: Location of the sensors on Tinajas Bridge.

Mode	f [Hz]	ξ [%]
1	3.0	0.7
2	3.7	0.6
3	6.0	0.4
4	10.5	0.6
5	11.7	0.5

Table 10: Identified natural frequencies of Tinajas Bridge: (red) span 2 and (blue) spans 1 and 3.

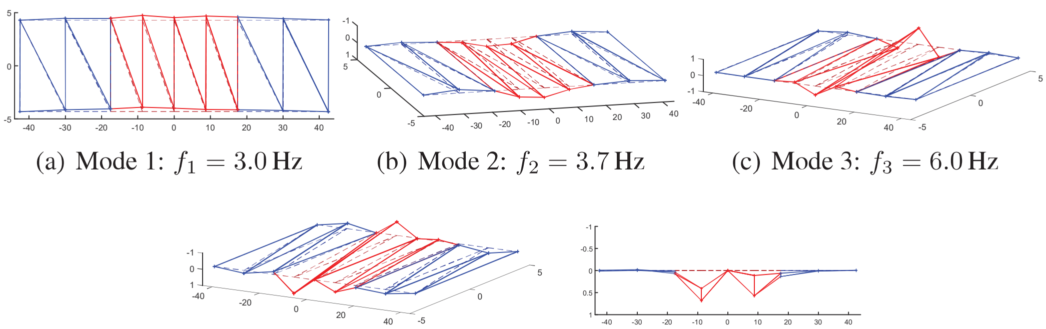

(a) Mode 1: $f_1 = 3.0\,\mathrm{Hz}$ (b) Mode 2: $f_2 = 3.7\,\mathrm{Hz}$ (c) Mode 3: $f_3 = 6.0\,\mathrm{Hz}$

(d) Mode 4: $f_4 = 10.5\,\mathrm{Hz}$ (e) Mode 5: $f_5 = 11.7\,\mathrm{Hz}$

Figure 30: Identified mode shapes of Tinajas Bridge: (blue) spans 1 and 3 and (blue) span 2.

3.5.1 Response due to ballast distributing and profiling and stabilisation machines passages

The objective of this test, unlike the previous, was to measure the bridge behaviour under track construction operations: ballast distribution, profiling and stabilisation . Plasser & Theurer Unimat 08-475/4S ballast distributing machine has two bogies with two axles separated $14\,\mathrm{m}$. The distance between axles is $1.8\,\mathrm{m}$ and the axle load is $198\,\mathrm{kN}$. Plasser & Theurer DGS

62N profiling and stabilisation machine consists of two bogies with two axles each one. The distance between bogies is $12\,\mathrm{m}$ and the distance between axles of the same bogie is $1.5\,\mathrm{m}$. The front axle load is $140\,\mathrm{kN}$ and the rear axle load is $145\,\mathrm{kN}$ in this case. The total load is approximately $570\,\mathrm{kN}$. Moreover, Plasser & Theurer DGS 62N applies a maximum vertical load of $356\,\mathrm{kN}$. Both machines are used to maintain the geometry and good condition of the track. The stabilization is done immediately after the tamping operations [15].

Figure 31 shows the longitudinal (x), lateral (y) and vertical (z) acceleration at points 4 and 11 due to the Plasser & Theurer DGS 62N operating at $40\,\mathrm{Hz}$ and the Plasser & Theurer Unimat 08-475/4S operating at $35\,\mathrm{Hz}$ with a nominal pressure of $20\,\mathrm{bar}$. The frequency content is represented in logarithmic scale. In the case of the profiling and stabilisation machine, the contribution of the load frequency can be clearly observed in the response.

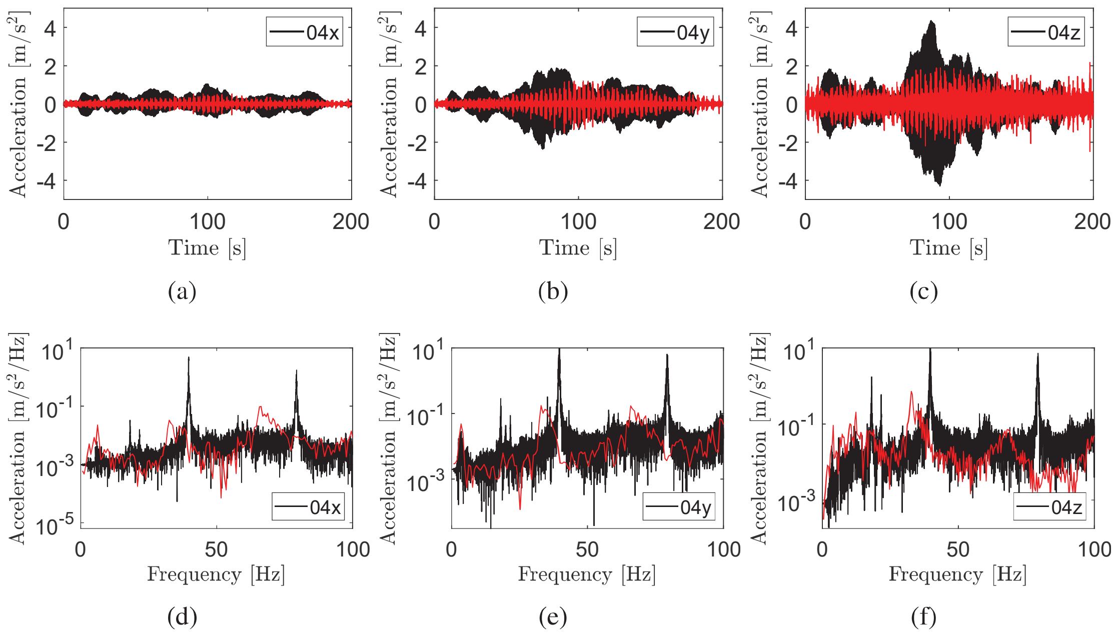

Figure 31: Tinajas bridge: (a-c) time history and (d-f) frequency content of the acceleration at point 4 induced by (black line) Plasser & Theurer DGS 62N profiling and stabilisation machine operating at $40\,\mathrm{Hz}$ and (red line) Plasser & Theurer Unimat 08-475/4S ballast distributing machine operating at $35\,\mathrm{Hz}$.

4 Conclusions

The experimental campaign presented in this paper is aimed at analysing the dynamic behaviour of railway bridges. The tests were performed on five bridges with different structural typologies: $i)$ a bridge with spans composed by two adjacent single-track decks sharing a continuous ballast track; $ii)$ a three-span bridge composed by a double-track pre-stressed concrete girders deck; $iii)$ a three-span S-S bridge with a filler-beam concrete deck; $iv)$ a three-span S-S steel truss bridge with a single ballastless track, and $v)$ a steel-concrete composite continuous three-span bridge. The bridge dynamic behaviour, the soil properties and the response under operational and maintenance conditions have been studied in the previous sections.

This work also shows that damping identification is difficult and depends on the chosen methodology. According to previous studies [8] it depends on the time span and bandpass filter applied but, despite that, it can be concluded that the estimated damping ratios in free vibration under operational conditions were always greater than the values obtained in ambient vibration.

The analysis of the acceleration response of the bridges due to train traffic shows, in the frequency domain, clear peaks associated to the excitation (bogie and axle passages, and even its corresponding harmonics) and also to the bridge lowest natural frequencies. The maximum overall acceleration measured is lower (yet significant), than the Serviceability Limit State prescribed by European Standards [12], limited to $3.5\,\mathrm{m/s^2}$ for bridges with ballasted tracks.

The coupling effect between adjacent decks of the same span caused by the continuity of the ballast layer is clearly perceptible in the train-induced vibrations of Old Guadiana bridge, which can be also identified under ambient vibrations. A similar observation was previously reported by Rauert at al. [16] in a S-S bridge formed by one span with two separated decks. Therefore, for an accurate prediction of the dynamic response of bridges composed by several S-S spans and/or structurally independent decks at each span, the consideration of the coupling effect induced by the ballast continuity in the numerical models may become important.

Acknowledgements

The acquisition of the experimental data on which this paper is based was made possible thanks to ADIF. The authors would like to acknowledge the financial support provided by (i) the Spanish Ministry of Economy and Competitiveness under the research project [BIA2016-75042-C2], (ii) the Spanish Ministries of Science, Innovation and Universities through the project US-126491 funded by the FEDER Andalucía 2014-2020 Operational Program, (iii) Generalitat Valenciana under the research project [AICO2019/175] and (iv) the Andalusian Scientific Computing Centre (CICA).

REFERENCES

[1] L. Frýba, Dynamic behaviour of bridges due to high-speed trains, in: Bridges for High-Speed Railways, CR Press, London, 2008, pp. 137–158.

[2] W. Hoorpah, Dynamic calculations of high-speed railway bridges in france – some case studies, in: Dynamics of High-Speed Railway Bridges, CR Press, London, 2008, pp. 133–145.

[3] M. Zacher, M. Baeßler, Dynamic behaviour of ballast on railway bridges, in: Dynamics of High-Speed Railway Bridges, CR Press, London, 2008, pp. 99–112.

[4] E. Reynders, System identification methods for (operational) modal analysis: Review and comparison, Archives of Computational Methods in Engineering 19 (1) (2012) 51–124. doi:10.1007/s11831-012-9069-x.

[5] S. A. Badsar, M. Schevenels, W. Haegeman, G. Degrande, Determination of the material damping ratio in the soil from SASW tests using the half-power bandwidth method, Geophysical Journal International 182 (3) (2010) 1493–1508. doi:10.1111/j.1365-246X.2010.04690.x.

[6] Renfe, Our trains.
URL https://www.renfe.com/EN/viajeros/nuestros_trenes/index.html

[7] CEN/TC250, Eurocode: Basis of structural design. Annex A2: Application for bridges. Final version, European Committee for Standardization, Brussels, 2005.

[8] B. H. Kim, N. Stubbs, T. Park, A new method to extract modal parameters using output-only responses, Journal of Sound and Vibration 282 (1) (2005) 215 – 230. doi:https://doi.org/10.1016/j.jsv.2004.02.026.

[9] M. Schevenels, S. François, G. Degrande, EDT: An elastodynamics toolbox for MATLAB, Computers & Geosciences 35 (8) (2009) 1752 – 1754. doi:http://dx.doi.org/10.1016/j.cageo.2008.10.012.

[10] A. Doménech, M. Martínez-Rodrigo, A. Romero, P. Galvín, On the basic phenomenon of soil-structure interaction on the free vibration response of beams: Application to railway bridges, Engineering Structures 125 (2016) 254 – 265. doi:http://dx.doi.org/10.1016/j.engstruct.2016.06.052.

[11] M. Martínez-Rodrigo, P. Galvín, A. Doménech, A. Romero, Effect of soil properties on the dynamic response of simply-supported bridges under railway traffic through coupled boundary element-finite element analyses, Engineering Structures 170 (2018) 78 – 90. doi:https://doi.org/10.1016/j.engstruct.2018.02.089.

[12] CEN, EN 1991-2, Eurocode 1: Actions on Structures - Part 2: Traffic loads on bridges, European Committee for Standardization, Brussels, 2002.

[13] Ministerio de transporte, turismo y comunicaciones, Nuevo acceso ferroviario a Andalucía. Tramo: Ciudad Real - Brazatortas. Proyecto de infraestructura y vía. Estudio geológico y geotécnico, Gobierno de España, 1987.

[14] Ministerio de transporte, turismo y comunicaciones, Proyecto de infraestructura y vía del tramo Mascaraque-El Emperador. Modificación nº 1. Documento nº 1. Memoria y anejos II., Gobierno de España, 1987.

[15] Indian Railways Institute of Civil Engineering, Mechanised Tamping & Stabilisation Pune - 411 001, Tech. rep. (November 2016).

[16] T. Rauert, H. Bigelow, B. Hoffmeister, M. Feldmann, On the prediction of the interaction effect caused by continuous ballast on filler beam railway bridges by experimentally supported numerical studies, Engineering Structures 32 (12) (2010) 3981–3988.